THE JOURNAL OF PHYSICAL CHEMISTRY Letters

pubs.acs.org/JPCL Letter

Theoretical and Spectroscopic Evidence of the Dynamic Nature of Copper Active Sites in Cu-CHA Catalysts under Selective Catalytic Reduction (NH_3–SCR–NO_x) Conditions

Reisel Millan, Pieter Cnudde, Alexander E. J. Hoffman, Christian W. Lopes, Patricia Concepción, Veronique van Speybroeck,* and Mercedes Boronat*

Cite This: *J. Phys. Chem. Lett.* 2020, 11, 10060–10066 Read Online

ACCESS | Metrics & More | Article Recommendations | Supporting Information

ABSTRACT: The dynamic nature of the copper cations acting as active sites for selective catalytic reduction of nitrogen oxides with ammonia is investigated using a combined theoretical and spectroscopic approach. Ab initio molecular dynamics simulations of Cu-CHA catalysts in contact with reactants and intermediates at realistic operating conditions show that only ammonia is able to release Cu^+ and Cu^{2+} cations from their positions coordinated to the zeolite framework, forming mobile $Cu^+(NH_3)_2$ and $Cu^{2+}(NH_3)_4$ complexes that migrate to the center of the cavity. Herein, we give evidence that such mobilization of copper cations modifies the vibrational fingerprint in the 800–1000 cm^{-1} region of the IR spectra. Bands associated with the lattice asymmetric T-O-T vibrations are perturbed by the presence of coordinated cations, and allow one to experimentally follow the dynamic reorganization of the active sites at operating conditions.

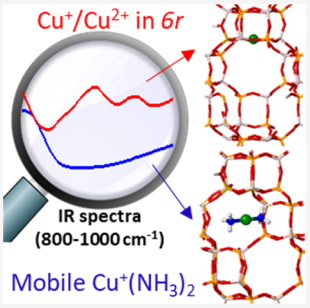

Removal of nitrogen oxides (NO_x) from exhaust gases in diesel vehicles is currently achieved through their selective catalytic reduction (SCR) with ammonia, the NH_3–SCR–NO_x reaction, using copper-exchanged zeolites, in particular, Cu-SSZ-13 and Cu-SAPO-34 with the CHA framework, as catalysts.[1−4] N_2 and H_2O are the harmless products formed by reaction of NO with NH_3 in the presence of either O_2 in the case of the standard SCR reaction or NO_2 in the so-called fast SCR reaction:

$$4NH_3 + 4NO + O_2 \rightarrow 4N_2 + 6H_2O$$

$$4NH_3 + 2NO + 2NO_2 \rightarrow 4N_2 + 6H_2O$$

Although the research effort devoted to this process in recent years has provided considerable understanding of the reaction mechanism in Cu-CHA catalysts,[5−15] there is still some uncertainty regarding the exact location of the active sites, the Cu^+ and Cu^{2+} cations, and their mobility as a function of oxidation state and reaction conditions, mainly temperature and gas feed composition. Herein, we give solid evidence for a unique vibrational fingerprint in the 800–1000 cm^{-1} region of the IR spectrum, which is associated with mobilized copper cations under reaction conditions.

The CHA framework is composed of hexagonal prisms or double 6-ring (*d6r*) units that link to form large cavities accessible through small 8-ring (*8r*) windows (Chart 1). Isolated Cu^{2+} cations preferentially occupy positions in the plane of the 6-ring (*6r*) units compensating two negative charges, while monovalent Cu^+ or $[Cu^{2+}(OH)^-]^+$ species can also be placed at the 8-ring (*8r*) windows.[15−19] Operando XAS and XES measurements during the NH_3–SCR–NO_x reaction have shown that at low temperature, up to ~473 K, NH_3 coordinates strongly to Cu^+ cations and releases them from their positions at the *6r* or *8r* rings to form mobile $Cu^+(NH_3)_2$ complexes.[10,15,20] Formation of transient $Cu^+(NH_3)_2$–O–O–$Cu^+(NH_3)_2$ dimeric species has been claimed as a key step in the low temperature oxidation of Cu^+ to Cu^{2+},[8−10] and

Chart 1. Illustration of the *cha* Cage Showing the *6r* and *8r*, a Cu^+ Cation in the *6r* and the Compensating Proton (a); Static DFT Optimized Geometry of Cu^+ and Cu^{2+} in the *6r* of Cu-SSZ-13 (b) and Cu-SAPO-34 (c)[a]

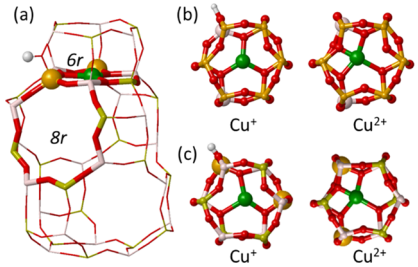

[a]Al, P, O, Si, Cu, and H atoms depicted in gray, yellow, red, orange, green, and white, respectively.

Received: October 3, 2020
Accepted: November 2, 2020
Published: November 12, 2020

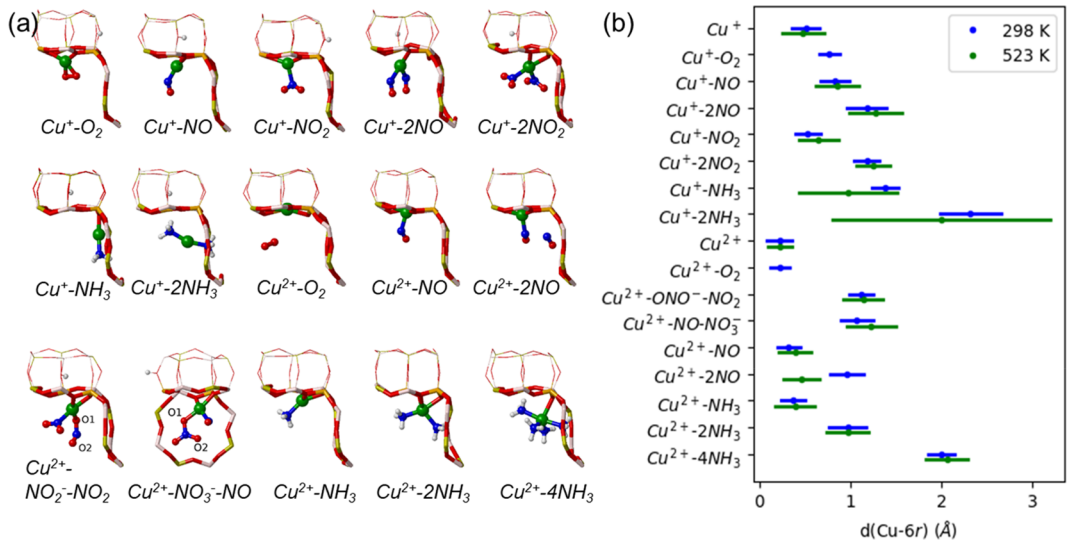

Figure 1. (a) Snapshots of the interaction of Cu^+ and Cu^{2+} cations in Cu-SAPO-34 with O_2, NO, NO_2, and NH_3 molecules and with nitrite and nitrate intermediates corresponding to geometries which are most frequently visited during AIMD runs of 100 ps at 298 K. (b) Overview of the average distances between Cu^+ or Cu^{2+} cations and the plane of the *6r* and root-mean-square deviations (RMSD) of the Cu^+ or Cu^{2+} position with respect to the ensemble average at 298 K (blue) and 523 K (green) in each system. Al, P, O, Si, Cu, N, and H atoms depicted in gray, yellow, red, orange, green, blue, and white, respectively.

experimental evidence of such dimer formation has been recently provided by XAS and diffuse reflectance UV−vis spectroscopies.[14] Alternatively, the oxidation of isolated, coordinated to the framework Cu^+ to Cu^{2+} in the absence of NH_3 was identified by EPR and IR spectroscopies in Cu-SSZ-13 and Cu-SAPO-34 catalysts at room temperature,[11] and similar activation energies have been reported for the two processes by means of DFT calculations.[11−13] These data indicate that there is not a unique clear picture of the state of copper cations in Cu-CHA catalysts under different reaction conditions at this moment, which inspired us to perform the current combined experimental/theoretical study to find a unique fingerprint for the state of copper under reaction conditions.

At first instance, to gain insight on the state and mobility of the active sites of Cu-CHA catalyst under different NH_3−SCR−NO_x reaction conditions, we studied the interaction of Cu^+ and Cu^{2+} cations in Cu-SSZ-13 and Cu-SAPO-34 catalyst models with the reactant molecules NO, O_2, NO_2, and NH_3, and with some relevant reaction intermediates found in our previous mechanistic study,[11] using *ab initio* molecular dynamics (AIMD) simulations at two different temperatures, 298 and 523 K. Figure 1 gives an overview of the average distances between Cu^+ or Cu^{2+} cations and the plane of the *6r* and the root-mean-square deviations (RMSD) of the Cu^+ or Cu^{2+} position with respect to the ensemble average in each system to enable a quantification of the cation mobility (see values in Table S1) and some representative snapshots during the AIMD simulations which were most frequently visited for Cu-SAPO-34. Similar snapshots for Cu-SSZ-13 are taken in Figure S1 of the SI. In the absence of adsorbed molecules, Cu^+ and Cu^{2+} cations are located in the plane of the *6r*, forming three or four strong bonds with the framework oxygen atoms of both Cu-SSZ-13 and Cu-SAPO-34 (Chart 1). The average Cu-*6r* distance is larger for Cu^+ than for Cu^{2+} in all cases, and the RMSD of Cu^+ increases at 523 K while that of Cu^{2+} remains smaller and constant, reflecting the stronger interaction of the divalent cation with the negatively charged framework.

The interaction of Cu^+ with one O_2, NO, or NO_2 molecule results in an adsorption state where the Cu^+ cation forms a new bond with an O or N atom of the adsorbed molecule, while it remains coordinated to two framework oxygen atoms of the *6r*, although somewhat displaced toward the cavity. Two guest NO and NO_2 molecules can also bind strongly to Cu^+ at 298 and 523 K leading to slightly larger average Cu-*6r* distances and increased mobility (RMSD) (Figures 1 and S1, and Table S1) but without detaching it from its position in the *6r*. The adsorption of NH_3 on Cu^+ modifies strongly its interaction with the catalyst framework so that NH_3 and Cu^+ move out of the plane of the *6r* and get close to the *8r*. Depending on the temperature and the number of NH_3 molecules present in the cages, the cation mobility increases significantly.

After adsorption of one NH_3 molecule in Cu-SAPO-34 at 298 K, the Cu^+ cation is slightly displaced from the *6r* but remains coordinated with a single oxygen of the *6r* while making a new coordination with NH_3, with an almost linear N−Cu−O geometry (Figure 2), in agreement with previous results on Cu-SSZ-13.[16] The mobility increases significantly at 523 K, allowing NH_3 and Cu^+ to diffuse through the *8r* window to the adjacent empty cage after ∼50 ps. Adsorption of a second NH_3 molecule breaks the last Cu−O bond present in the Cu^+−NH_3 system, and a linear $Cu^+(NH_3)_2$ complex placed freely in the cavity is obtained. At 298 K, the complex forms as soon as the two NH_3 molecules approach the Cu^+ cation and remains stable during the whole simulation. At this temperature, the complex remains relatively close to the *6r* due to the electrostatic interaction between Cu^+ and the negatively charged oxygen atoms of the framework (Cu-*6r* distance and its RMSD value are also tabulated in Table S1). At 523 K, the mobility of the $Cu^+(NH_3)_2$ complex increases substantially, and after 50 ps, it diffuses through the *8r* window to the adjacent empty cavity while remaining close to the negatively charged framework (Figure 2).

https://dx.doi.org/10.1021/acs.jpclett.0c03020
J. Phys. Chem. Lett. 2020, 11, 10060−10066

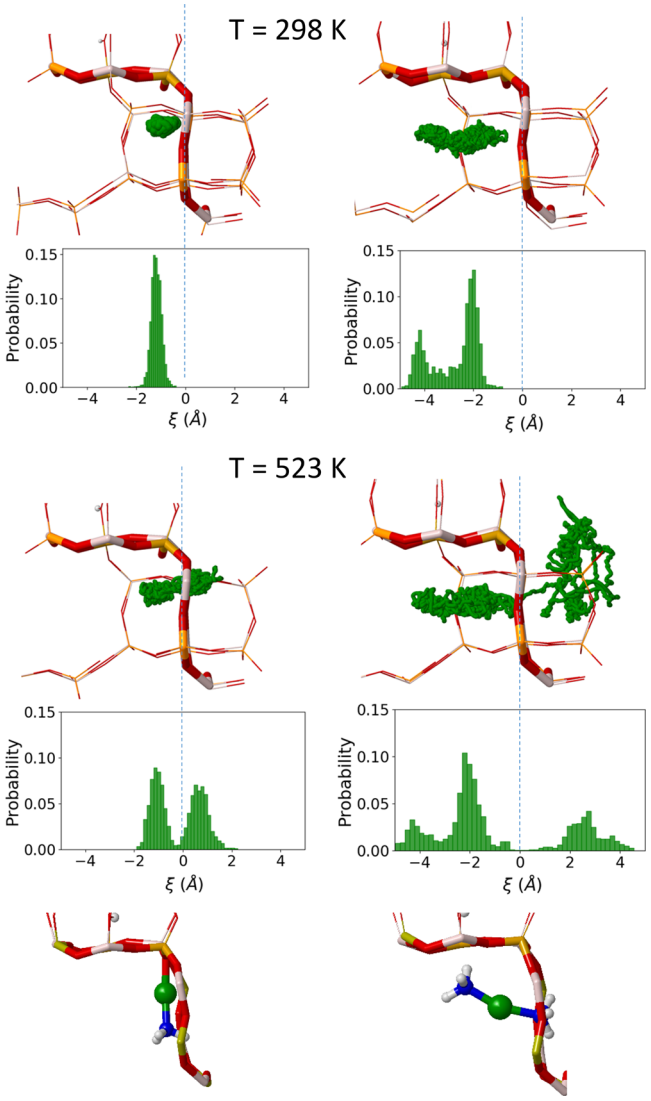

Figure 2. Scatter plot of the position of Cu^+ in the SAPO-34 cavity and probability distributions of the Cu-*8r* distance in AIMD simulations obtained over a 100 ps run for the interaction of Cu^+ with one (left) and two (right) NH_3 molecules at 298 and 523 K. Snapshots of the complexes are also shown. The ξ-axis represents the projection of the position of Cu^+ on the vector normal to the average plane of the *8r*.[25] The centroid of the *8r* is the reference coordinate such that when Cu^+ is in the center of the *8r*, ξ is equal to 0, indicated with a slashed vertical line.

In the next step, we determined the effect of the oxidation state of copper on the mobility of Cu^{2+} cations interacting with O_2, NO, and NH_3, which is further stabilized by two negative charges in the *6r*. Molecular O_2 does not bind to Cu^{2+}, and only one NO molecule can interact with Cu^{2+} forming a stable system that only displaces slightly the Cu^{2+} cation out of the *6r* plane (Figures 1 and S1). Two NH_3 can bind to Cu^{2+}, but the interaction is not strong enough to break the Cu−O bonds, and therefore, the Cu^{2+} cation remains in the *6r* plane, although with a high mobility (see RMSD values in Table S1 of the SI). Four NH_3 molecules are able to detach Cu^{2+} out of the *6r* and form a square planar $Cu^{2+}(NH_3)_4$ complex that remains stable in the cavity both at 298 and 523 K (Figures 1 and S1).

Nitrites and nitrates formed from NO and O_2 following our previous proposal[11] could also modify the state of copper under NH_3−SCR−NO_x reaction conditions, and therefore two additional systems containing a NO_2 molecule and a nitrite anion NO_2^- attached to copper (Cu^{2+}−NO_2^-−NO_2) and nitrate coadsorbed with NO (Cu^{2+}−NO_3^-−NO) were also considered (Figures 1 and S1, and Table S1). The evolution of some of the Cu−O distances during the simulations indicates that both nitrite and NO_2 interact strongly with Cu^{2+} and that the Cu−O bonds are quite dynamic, especially at 523 K. Thus, the original Cu−O1 bond in the nitrite anion is broken after some time and a new bond appears between Cu^{2+} and the equivalent O2 atom (Figure S2a). A similar dynamic behavior, with an interchange of the Cu−O1 and Cu−O2 bonds, was also observed for nitrate NO_3^- coadsorbed with NO (Figure S2b). In summary, the AIMD simulations indicate that Cu^+ and Cu^{2+} usually reside close to the *6r* plane interacting with framework oxygen atoms, and only NH_3 is able to mobilize them by forming $Cu^+(NH_3)_2$ or $Cu^{2+}(NH_3)_4$ complexes.

Having obtained insight into the mobility of Cu^+ and Cu^{2+} cations in contact with reactants and intermediates using AIMD simulations, we analyzed in a next step the IR spectrum of Cu-SAPO-34 exposed to different combinations of reactants and temperatures to investigate whether a vibrational fingerprint could be found for mobile copper cations under reaction conditions. As reported earlier, IR spectra of Cu-CHA and other Cu-containing zeolite catalysts exhibit some bands in the 800−1000 cm^{-1} region associated with the framework asymmetric T-O-T vibrations perturbed by the presence of coordinated cations.[21−24] Herein, the ν_{asym}(T-O-T) region of the IR spectra of Cu-SAPO-34 exposed to different reactant feeds and temperatures was analyzed in detail, assisted by theoretical vibrational spectra computed with both static and dynamic based approaches (see Table 1 and Figures 3, S3, and S4).

Table 1. Vibrational Frequencies (in cm^{-1}) between 800 and 1000 cm^{-1} Calculated for Cu-SAPO-34 with Static DFT and from AIMD Simulations at 298 K

	static DFT	AIMD
Cu^+	983, 964, 877	910, 817
Cu^{2+}	960, 900, 874, 835	888, 876, 833
Cu^+−O_2	985, 816	862, 850
Cu^+−NO	972, 894	920, 888, 855
Cu^+−2NO	953, 892	-
Cu^+−NO_2	961, 885	916, 840
Cu^+−$2NO_2$	935, 865, 808	888, 812
Cu^+−NH_3	969, 905	920, 835
Cu^+−$2NH_3$	984, 964	-
Cu^{2+}−ONO−NO_2	934, 875, 860	932, 895, 820
Cu^{2+}−NO_3−NO	993, 968, 873	930, 868, 815
Cu^{2+}−NO_3	946, 861	850
Cu^{2+}−2NO	992, 984, 948, 883	900
Cu^{2+}−$2NH_3$	990, 921, 859	900, 868
Cu^{2+}−$4NH_3$	997	-

The IR spectra of the parent H-SAPO-34 catalyst and of Cu-SAPO-34 activated either in vacuum at 723 K (containing predominantly Cu^+) or in O_2 at 623 K (containing predominantly Cu^{2+})[15−17] (Figure 3a) were used as reference to check the accuracy of the calculated spectra (see details in the Supporting Information). There is a very good agreement between the experimental and the simulated spectra for H-SAPO-34, with absence of peaks in both cases. For Cu^{2+} in Cu-

https://dx.doi.org/10.1021/acs.jpclett.0c03020
J. Phys. Chem. Lett. 2020, 11, 10060−10066

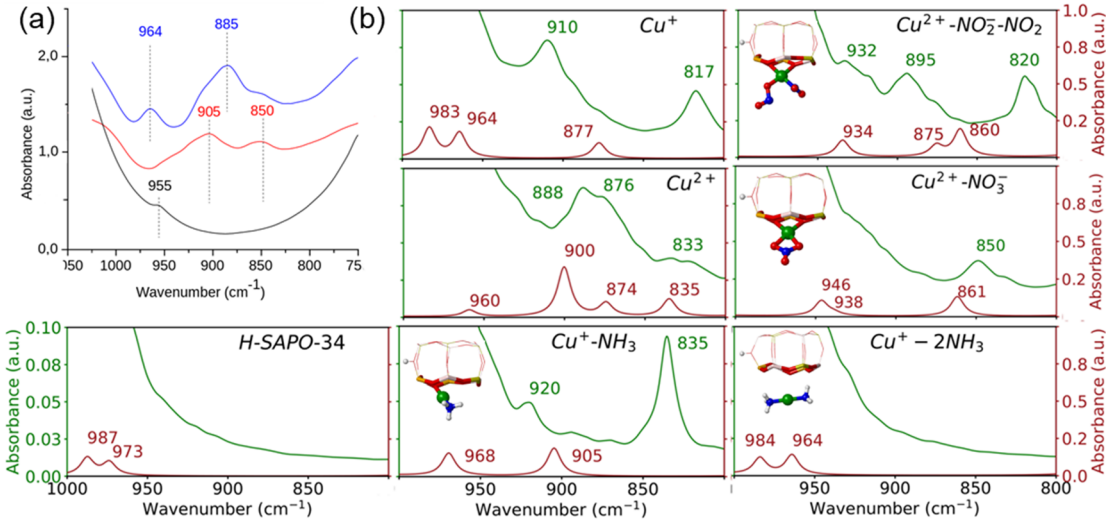

Figure 3. (a) Vibrational ν_{asym}(T-O-T) region of the FTIR spectra of H-SAPO-34 (black line) and Cu-SAPO-34 preactivated in vacuum at 723 K (redline) or in O_2 at 623 K followed by vacuum at 523 K (blueline). (b) Simulated vibrational spectra in the same region obtained from static DFT (red lines) and AIMD calculations at 298 K (green lines).

Scheme 1. Summary of Copper Species Identified by EXAFS (in Red) and IR (in Blue) Spectroscopies in Cu-SAPO-34 Samples Exposed to Different Reaction Conditions, Indicating the Presence or Absence of T-O-T Vibrations in the 800−1000 cm^{-1} IR Region

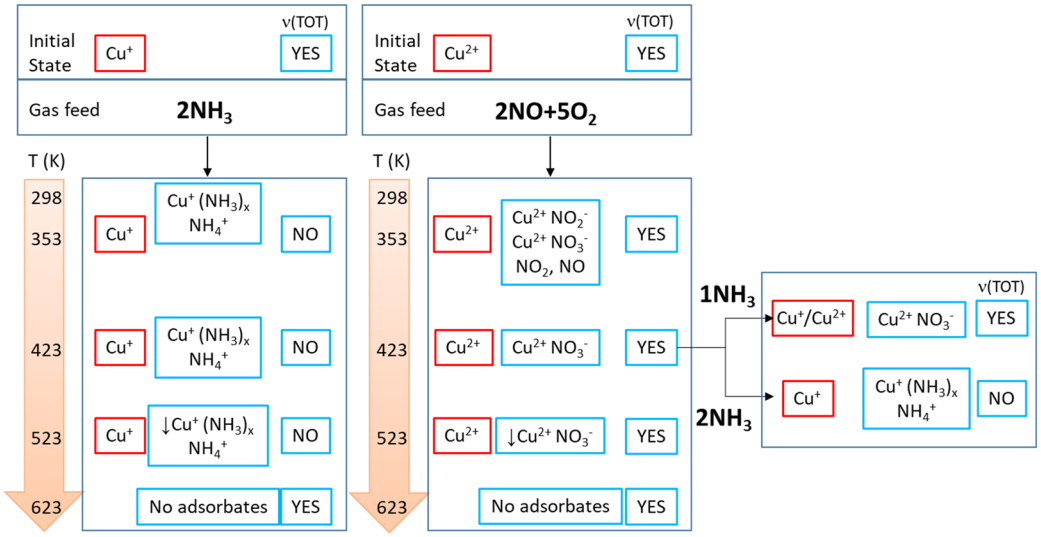

SAPO-34, the experimental peak at ~960 cm^{-1}, the intense and broad band at ~890 cm^{-1}, and the less intense signal at ~840 cm^{-1} are also well reproduced by the simulations (Table 1 and Figure 3). The higher mobility of Cu^+ in the *6r* of Cu-SAPO-34 discussed before makes the static DFT frequencies less reliable, and the band at ~905 cm^{-1} in the IR spectrum of Figure 3a (redline) is only well reproduced by the AIMD simulations.

The interaction of Cu^+ and Cu^{2+} cations with reactant and intermediate species modifies the calculated vibrational frequencies in the 800−1000 cm^{-1} region as a consequence of the displacement of the copper cations from the *6r* plane and the rupture of some of the Cu−O bonds, and both the static DFT and the AIMD data indicate that bands around ~850 and ~890 cm^{-1} should be visible in the IR spectra when NO_2, nitrite, or nitrate intermediates are adsorbed on the Cu^+ or Cu^{2+} cations (Table 1 and Figures 3 and S4).

Regarding NH_3 adsorption, the high mobility of Cu^+−NH_3 complexes makes the spectra obtained from static and dynamic approaches quite different (Figure 3b) with a big band at 835 cm^{-1} being predicted only by AIMD simulations. When two NH_3 molecules adsorb simultaneously on Cu^+, a linear $Cu^+(NH_3)_2$ species is formed that moves to the center of the cage. In this situation, there are no direct bonds between Cu^+ and the framework oxygen atoms, and therefore no bands in the 800−1000 cm^{-1} region associated with perturbations of the framework T-O-T vibrations are obtained. A similarly flat spectrum is obtained for the $Cu^{2+}(NH_3)_4$ complex placed in the cavity. However, for the still coordinated to the *6r* Cu^{2+}−$2NH_3$ structure, features at ~900 and ~860 cm^{-1} are observed in both spectra (see Table 1). These data indicate that a direct assignation of each vibrational frequency to a particular species is not possible, but suggest that broad bands around ~890 cm^{-1} could be associated with Cu^{2+} attached to NO_2, nitrite or nitrate intermediates, and confirm that no bands in the 800−

https://dx.doi.org/10.1021/acs.jpclett.0c03020
J. Phys. Chem. Lett. 2020, 11, 10060−10066

1000 cm^{-1} region should be observed when copper cations are not directly coordinated to the framework oxygen atoms.

Then, the Cu-SAPO-34 sample was exposed to different combinations of reactants NO, O_2, and NH_3 at increasing temperatures, and characterized by means of X-ray absorption and FTIR spectroscopies, as outlined in Scheme 1. The frequency region of the IR spectra between 800 and 1000 cm^{-1} was analyzed in detail taking into account the simulations described before, the XAS data (Tables 2, S2, Figures S5−S7, and detailed description in the SI) and the information provided by the bands observed simultaneously between 1300 and 2000 cm^{-1} (Figures 4 and S8−S11).

Table 2. Oxidation State and Coordination Environment of Copper in Cu-SAPO-34 Catalyst Obtained from Linear Combination Fit (LCF) (Figure S6) and from Analysis of the k^2-Weighted EXAFS Data (Table S2 and Figure S7) at Different Reaction Conditions

reaction condition	temperature (K)	Cu^+ (%)	Cu^{2+} (%)	N[a]	r[b] (Å)
2NO + 0.5NH_3	353	35	65	3.2	1.940
	423	92	8	1.7	1.882
	523	100	0	1.6	1.879
2NO + 5O_2	353	0	100	3.9	1.915
	423	0	100	3.9	1.912
	523	0	100	3.9	1.913
2NO + 0.5NH_3 + 5O_2	353	0	100	3.6	1.926
	423	65	35	2.5	1.890
	523	45	55	2.9	1.902

[a]Coordination number. [b]Average distance over the first coordination shell.

To ensure the possibility of migration of the copper cations, a Cu-SAPO-34 sample preactivated in vacuum was used in the IR study of NH_3 adsorption. IR bands at 850 and 910 cm^{-1} associated with Cu^+ in the *6r* are clearly observed before NH_3 adsorption (Figures 4a and S8, black line), which completely disappear after addition of 2NH_3/Cu at 298 K (Figures 4a and S8, blue line), confirming the migration of Cu^+ to the cavity as proposed by the AIMD simulations. Raising temperature in the closed IR cell (green and pink lines in Figures 4a and S8) leads to a decrease in the intensity of the band at 1620 cm^{-1} attributed to NH_3 adsorbed on Lewis acid sites, but only after vacuum at 623 K (red line) NH_3 is detached from Cu^+ ions and the bands at ∼910 and ∼850 cm^{-1} are recovered, indicating that copper cations have returned to their position in the *6r*.

Next, a Cu-SAPO-34 sample preactivated in O_2 and exhibiting lattice vibrational bands associated with Cu^{2+} (965 and 885 cm^{-1}) and Cu^+ (910 and 855 cm^{-1}) (Figures 4b and S9a, black line) was exposed to 2NO/5O_2/Cu at 298 K (Figures 4b and S9a, navy line). IR bands associated with NO, NO_2, nitrites, and nitrates are observed in the high frequency region (see details in the Supporting Information); and simultaneously, in the lattice vibrations frequency region, the IR peak at 965 cm^{-1} disappears, the signals at ∼910 and 855 cm^{-1} decrease, and a broad band grows around 885 cm^{-1}. Based on the simulated spectra previously discussed and the XAS data in Table 2 indicating that only Cu^{2+} coordinated to the framework and directly bonded to four O atoms is present under these conditions, this broad band is assigned to Cu^{2+} in the *6r* interacting with NO_2, nitrites, and nitrates. These species are stable at 423 K and only start to desorb or decompose at higher temperatures (Figure S9b).

To study the mobilizing effect of NH_3, controlled amounts of NH_3 were added to a Cu-SAPO-34 sample previously exposed to 2NO/5O_2 at 423 K (Figures 4c and S10, green line) that contains NO_2, nitrites, and nitrates bonded to Cu^{2+}. The XAS study indicates that the addition of a small amount of

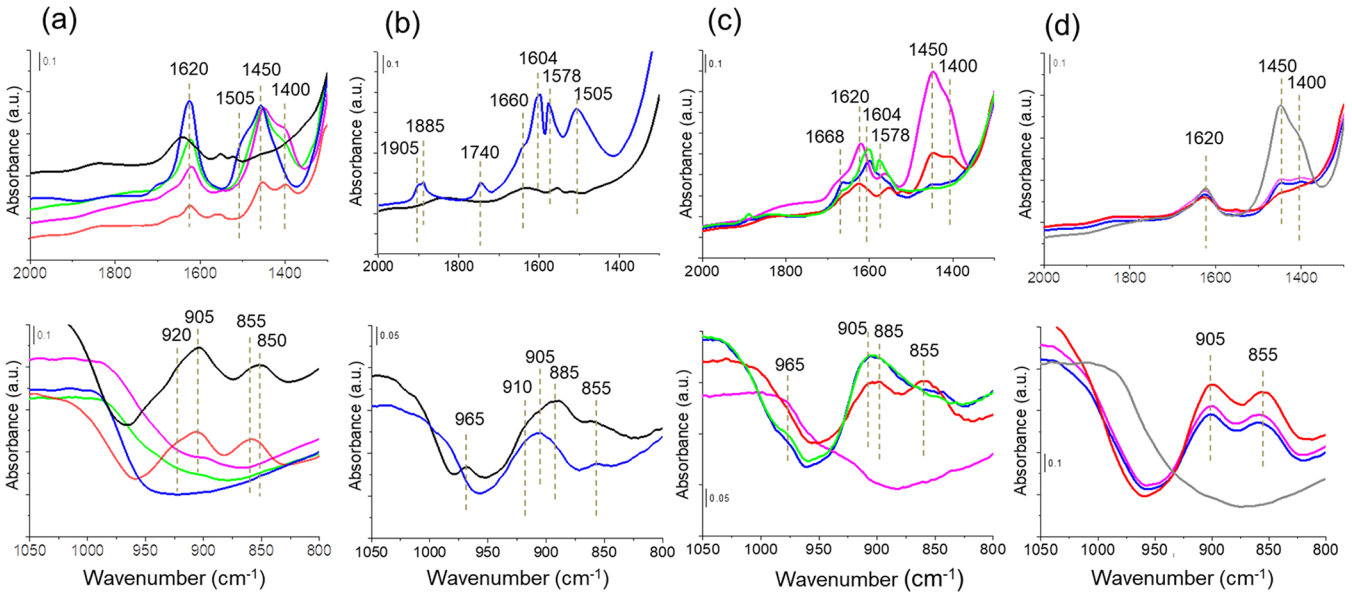

Figure 4. FTIR spectra of Cu-SAPO-34 before (black lines) and after adsorption of different reactant mixtures. (a) 2NH_3/Cu at 298 K (blue line) and increasing temperature to 423 K (green line), 523 K (pink line), and 623 K (red line). (b) 2NO/5O_2/Cu at 298 K (blue line). (c) 2NO/5O_2/Cu at 423 K (green line) followed by addition of 1NH_3/Cu (blue line) and 2NH_3/Cu (pink line) at 423 K and further increasing temperature to 523 K (red line). (d) 2NO/2NH_3/Cu at 523 K (gray line) followed by addition of 5O_2/Cu at 523 K (blue line) and increasing temperature to 573 K (pink line) and 623 K (red line). Prior to adsorption, the sample was preactivated in vacuum at 723 K for 2 h (a) or in O_2 at 623 K for 2 h, followed by vacuum at 423 K for 1 h (b, c, and d).

https://dx.doi.org/10.1021/acs.jpclett.0c03020
J. Phys. Chem. Lett. 2020, 11, 10060−10066

NH_3 together with NO and O_2 leads to a reduction of 65% of Cu^{2+} to Cu^+ (see Table 2). Addition of $1NH_3$/Cu at 423 K does not cause relevant changes in the IR spectrum, indicating that both Cu^+ and Cu^{2+} cations remain coordinated to the framework oxygen atoms (blue line in Figures 4c and S10). In contrast, addition of $2NH_3$/Cu at 423 K (pink line in Figures 4c and S10) causes the disappearance of all IR signals in the 800−1000 cm^{-1} region, in agreement with the results from the AIMD simulations. At 523 K (red line), the adsorbed intermediates decompose and two bands centered at ∼900 and ∼850 cm^{-1} appear again, indicating the reallocation of copper cations in the *6r* units of the SAPO-34 framework.

Finally, the Cu-SAPO-34 sample was first exposed to 2NO/$2NH_3$/Cu at 523 K to ensure the reduction of all Cu^{2+} to Cu^+ (see Table 2) and the total migration of Cu^+ cations to the cavity in the form of $Cu^+(NH_3)_2$ complexes, as confirmed by the absence of IR bands in the 800−1000 cm^{-1} region (Figures 4d and S11, gray line). After addition of $5O_2$/Cu at 523 K (Figures 4d and S11, blue line) the NH_4^+ cations and NH_3 bonded to Lewis sites are consumed, while the bands centered at ∼900 and ∼850 cm^{-1} appear, indicating a the return of copper cations to the *6r* of the SAPO-34 framework.

To summarize, the dynamic behavior of copper cations in Cu-SAPO-34 catalyst under NH_3−SCR−NO_x reaction conditions has been investigated in detail by combining static DFT, AIMD simulations, and XAS and IR spectroscopies. The AIMD simulations show that only the interaction with NH_3 is able to break the coordination of Cu^+ and Cu^{2+} cations to the framework oxygen atoms, resulting in the formation of mobile $Cu^+(NH_3)_2$ and $Cu^{2+}(NH_3)_4$ complexes that migrate to the *cha* cavity. Computationally assisted analysis of the 800−1000 cm^{-1} region of the IR spectra of Cu-SAPO-34 exposed to different reactant mixtures and temperatures confirms that complete migration of copper cations from the *6r* to the cavity only occurs when there is enough NH_3 present in the reaction media, and that reaction of $Cu^+(NH_3)_2$ complexes with added O_2 leads to a fast recovering of the peaks in the 800−1000 cm^{-1} IR region, indicating the return of copper cations to the *6r* of the SAPO-34 framework. The complementary experimental and computational approach allows one to observe the dynamic reorganization of the catalytic active sites for the SCR−NO_x reaction, and could be applied to follow *in situ* and *operando* whether the complete catalytic cycle of the SCR−NO_x reaction occurs in the cavity or if some elementary steps occur necessarily on copper cations coordinated to framework oxygens.

■ ASSOCIATED CONTENT

Supporting Information

The Supporting Information is available free of charge at https://pubs.acs.org/doi/10.1021/acs.jpclett.0c03020.

Experimental Section, cation mobility in Cu-SSZ-13 from AIMD simulations, vibrational spectra from static DFT and AIMD simulations, characterization by EXAFS spectroscopy, characterization by IR spectroscopy (PDF)

■ AUTHOR INFORMATION

Corresponding Authors

Mercedes Boronat − *Instituto de Tecnología Química, Universitat Politècnica de València-Consejo Superior de Investigaciones Científicas, 46022 València, Spain;* orcid.org/0000-0002-6211-5888; Email: boronat@itq.upv.es

Veronique van Speybroeck − *Center for Molecular Modeling, Ghent University, 9052 Zwijnaarde, Belgium;* orcid.org/0000-0003-2206-178X; Email: veronique.vanspeybroeck@ugent.be

Authors

Reisel Millan − *Instituto de Tecnología Química, Universitat Politècnica de València-Consejo Superior de Investigaciones Científicas, 46022 València, Spain;* orcid.org/0000-0002-4489-5411

Pieter Cnudde − *Center for Molecular Modeling, Ghent University, 9052 Zwijnaarde, Belgium;* orcid.org/0000-0002-6735-0078

Alexander E. J. Hoffman − *Center for Molecular Modeling, Ghent University, 9052 Zwijnaarde, Belgium;* orcid.org/0000-0002-1529-4705

Christian W. Lopes − *Laboratório de Reatividade e Catálise (LRC), Universidade Federal do Rio Grande do Sul, 91501-970 Porto Alegre, Brazil;* orcid.org/0000-0001-8420-1958

Patricia Concepción − *Instituto de Tecnología Química, Universitat Politècnica de València-Consejo Superior de Investigaciones Científicas, 46022 València, Spain;* orcid.org/0000-0003-2058-3103

Complete contact information is available at: https://pubs.acs.org/10.1021/acs.jpclett.0c03020

Notes

The authors declare no competing financial interest.

■ ACKNOWLEDGMENTS

This work has been supported by the European Union through ERC-AdG-2014-671093 (SynCatMatch), Spanish Government through "Severo Ochoa" (SEV-2016-0683, MINECO), and MAT2017-82288-C2-1-P (AEI/FEDER, UE). Red Española de Supercomputación (RES) and Servei d'Informàtica de la Universitat de València (SIUV) are acknowledged for computational resources and technical support. R.M. thanks ITQ for his contract. V.V.S. and P.C. acknowledge funding from the European Union's Horizon 2020 research and innovation program (consolidator ERC grant agreement No. 647755 - DYNPOR (2015−2020)). V.V.S. acknowledges the Research Board of the Ghent University (BOF). The computational resources and services used were provided by Ghent University (Stevin Supercomputer Infrastructure), the VSC (Flemish Supercomputer Center), funded by the Research Foundation - Flanders (FWO).

■ REFERENCES

(1) Chen, H.-Y. Cu/Zeolite SCR Catalysts for Automotive Diesel NOx Emission Control. In *Urea-SCR Technology for deNOx After Treatment of Diesel Exhausts*, Nova, I.; Tronconi, E., Eds.; Fundamental and Applied Catalysis; Springer: New York, NY, 2014; pp 123−147.

(2) Beale, A. M.; Gao, F.; Lezcano-Gonzalez, I.; Peden, C. H. F.; Szanyi, J. Recent Advances in Automotive Catalysis for NOx Emission Control by Small-Pore Microporous Materials. *Chem. Soc. Rev.* **2015**, *44*, 7371−7405.

(3) Zhang, R.; Liu, N.; Lei, Z.; Chen, B. Selective Transformation of Various Nitrogen-Containing Exhaust Gases toward N2 over Zeolite Catalysts. *Chem. Rev.* **2016**, *116*, 3658−3721.

(4) Peden, C. H. F. Cu/Chabazite Catalysts for 'Lean-Burn' Vehicle Emission Control. *J. Catal.* **2019**, *373*, 384−389.
(5) Paolucci, C.; Verma, A. A.; Bates, S. A.; Kispersky, V. F.; Miller, J. T.; Gounder, R.; Delgass, W. N.; Ribeiro, F. H.; Schneider, W. F. Isolation of the Copper Redox Steps in the Standard Selective Catalytic Reduction on Cu-SSZ-13. *Angew. Chem., Int. Ed.* **2014**, *53*, 11828−11833.
(6) Janssens, T. V. W.; Falsig, H.; Lundegaard, L. F.; Vennestrom, P. N. R.; Rasmussen, S. B.; Moses, P. G.; Giordanino, F.; Borfecchia, E.; Lomachenko, K. A.; Lamberti, C.; et al. A Consistent Reaction Scheme for the Selective Catalytic Reduction of Nitrogen Oxides with Ammonia. *ACS Catal.* **2015**, *5*, 2832−2845.
(7) Jones, C. B.; Khurana, I.; Krishna, S. H.; Shih, A. J.; Delgass, W. N.; Miller, J. T.; Ribeiro, F. H.; Schneider, W. F.; Gounder, R. Effects of Dioxygen Pressure on Rates of NOx Selective Catalytic Reduction with NH3 on Cu-CHA Zeolites. *J. Catal.* **2020**, *389*, 140−149.
(8) Gao, F.; Mei, D.; Wang, Y.; Szanyi, J.; Peden, C. H. F. Selective Catalytic Reduction over Cu/SSZ-13: Linking Homo- and Heterogeneous Catalysis. *J. Am. Chem. Soc.* **2017**, *139*, 4935−4942.
(9) Paolucci, C.; Khurana, I.; Parekh, A. A.; Li, S.; Shih, A. J.; Li, H.; Iorio, J. R. D.; Albarracin-Caballero, J. D.; Yezerets, A.; Miller, J. T.; et al. Dynamic Multinuclear Sites Formed by Mobilized Copper Ions in NOx Selective Catalytic Reduction. *Science* **2017**, *357*, 898−903.
(10) Paolucci, C.; Di Iorio, J. R.; Schneider, W. F.; Gounder, R. Solvation and Mobilization of Copper Active Sites in Zeolites by Ammonia: Consequences for the Catalytic Reduction of Nitrogen Oxides. *Acc. Chem. Res.* **2020**, *53*, 1881−1892.
(11) Moreno-González, M.; Millán, R.; Concepción, P.; Blasco, T.; Boronat, M. Spectroscopic Evidence and Density Functional Theory (DFT) Analysis of Low-Temperature Oxidation of Cu^{+} to Cu^{2+} NO_x in Cu-CHA Catalysts: Implications for the SCR−NO x $_{Re}$action Mechanism. *ACS Catal.* **2019**, *9*, 2725−2738.
(12) Chen, L.; Falsig, H.; Janssens, T. V. W.; Grönbeck, H. Activation of Oxygen on (NH3CuNH3)+ in NH3-SCR over Cu-CHA. *J. Catal.* **2018**, *358*, 179−186.
(13) Chen, L.; Janssens, T. V. W.; Vennestrøm, P. N. R.; Jansson, J.; Skoglundh, M.; Grönbeck, H. A Complete Multisite Reaction Mechanism for Low-Temperature NH3-SCR over Cu-CHA. *ACS Catal.* **2020**, *10*, 5646−5656.
(14) Negri, C.; Selleri, T.; Borfecchia, E.; Martini, A.; Lomachenko, K. A.; Janssens, T. V. W.; Cutini, M.; Bordiga, S.; Berlier, G. Structure and Reactivity of Oxygen-Bridged Diamino Dicopper(II) Complexes in Cu-Ion-Exchanged Chabazite Catalyst for NH3-Mediated Selective Catalytic Reduction. *J. Am. Chem. Soc.* **2020**, *142*, 15884−15896.
(15) Borfecchia, E.; Beato, P.; Svelle, S.; Olsbye, U.; Lamberti, C.; Bordiga, S. Cu-CHA − a Model System for Applied Selective Redox Catalysis. *Chem. Soc. Rev.* **2018**, *47*, 8097−8133.
(16) Giordanino, F.; Borfecchia, E.; Lomachenko, K. A.; Lazzarini, A.; Agostini, G.; Gallo, E.; Soldatov, A. V.; Beato, P.; Bordiga, S.; Lamberti, C. Interaction of NH3 with Cu-SSZ-13 Catalyst: A Complementary FTIR, XANES, and XES Study. *J. Phys. Chem. Lett.* **2014**, *5*, 1552−1559.
(17) Borfecchia, E.; Lomachenko, K. A.; Giordanino, F.; Falsig, H.; Beato, P.; Soldatov, A. V.; Bordiga, S.; Lamberti, C. Revisiting the Nature of Cu Sites in the Activated Cu-SSZ-13 Catalyst for SCR Reaction. *Chem. Sci.* **2015**, *6*, 548−563.
(18) Lezcano-Gonzalez, I.; Deka, U.; Arstad, B.; Van Yperen-De Deyne, A.; Hemelsoet, K.; Waroquier, M.; Van Speybroeck, V.; Weckhuysen, B. M.; Beale, A. M. Determining the Storage, Availability and Reactivity of NH3 within Cu-Chabazite-Based Ammonia Selective Catalytic Reduction Systems. *Phys. Chem. Chem. Phys.* **2014**, *16*, 1639−1650.
(19) Martini, A.; Borfecchia, E.; Lomachenko, K. A.; Pankin, I. A.; Negri, C.; Berlier, G.; Beato, P.; Falsig, H.; Bordiga, S.; Lamberti, C. Composition-Driven Cu-Speciation and Reducibility in Cu-CHA Zeolite Catalysts: A Multivariate XAS/FTIR Approach to Complexity. *Chem. Sci.* **2017**, *8*, 6836−6851.
(20) Lomachenko, K. A.; Borfecchia, E.; Negri, C.; Berlier, G.; Lamberti, C.; Beato, P.; Falsig, H.; Bordiga, S. The Cu-CHA DeNO(x) Catalyst in Action: Temperature-Dependent NH3-Assisted Selective Catalytic Reduction Monitored by Operando XAS and XES. *J. Am. Chem. Soc.* **2016**, *138*, 12025−12028.
(21) Kwak, J. H.; Varga, T.; Peden, C. H. F.; Gao, F.; Hanson, J. C.; Szanyi, J. Following the Movement of Cu Ions in a SSZ-13 Zeolite during Dehydration, Reduction and Adsorption: A Combined in Situ TP-XRD, XANES/DRIFTS Study. *J. Catal.* **2014**, *314*, 83−93.
(22) Luo, J.; Gao, F.; Kamasamudram, K.; Currier, N.; Peden, C. H. F.; Yezerets, A. New Insights into Cu/SSZ-13 SCR Catalyst Acidity. Part I: Nature of Acidic Sites Probed by NH3 Titration. *J. Catal.* **2017**, *348*, 291−299.
(23) Song, J.; Wang, Y.; Walter, E. D.; Washton, N. M.; Mei, D.; Kovarik, L.; Engelhard, M. H.; Prodinger, S.; Wang, Y.; Peden, C. H. F.; et al. Toward Rational Design of Cu/SSZ-13 Selective Catalytic Reduction Catalysts: Implications from Atomic-Level Understanding of Hydrothermal Stability. *ACS Catal.* **2017**, *7*, 8214−8227.
(24) Martini, A.; Signorile, M.; Negri, C.; Kvande, K.; Lomachenko, K. A.; Svelle, S.; Beato, P.; Berlier, G.; Borfecchia, E.; Bordiga, S. EXAFS wavelet transform analysis of Cu-MOR zeolites for the direct methane to methanol conversion. *Phys. Chem. Chem. Phys.* **2020**, *22*, 18950−18963.
(25) Cnudde, P.; Demuynck, R.; Vandenbrande, S.; Waroquier, M.; Sastre, G.; Speybroeck, V. V. Light Olefin Diffusion during the MTO Process on H-SAPO-34: A Complex Interplay of Molecular Factors. *J. Am. Chem. Soc.* **2020**, *142*, 6007−6017.

https://dx.doi.org/10.1021/acs.jpclett.0c03020
J. Phys. Chem. Lett. 2020, 11, 10060−10066